Studies on mechanisms of the rearrangement of thieno[3,2-*e*][1,2,4]triazolo[4,3-*c*]pyrimidines into thieno[3,2-*e*][1,2,4]triazolo[1,5-*c*]pyrimidines

E. V. Vorob´ev,[a] M. E. Kletskii,[b] V. V. Krasnikov,[a] V. V. Mezheritskii,[a] and D. V. Steglenko[b]*

[a]Institute of Physical and Organic Chemistry, Rostov State University, 194/2 prosp. Stachki, 344090 Rostov-on-Don, Russian Federation. Fax: +7 (863) 243 4667. E-mail: mezher@ipoc.rsu.ru
[b]Department of Chemistry, Rostov State University, 7 ul. Zorge, 344090 Rostov-on-Don, Russian Federation

Recyclization of thieno[3,2-*e*][1,2,4]triazolo[4,3-*c*]pyrimidines was studied experimentally and theoretically by B3LYP/6-31G** calculations in the gas phase and in solution (EtOH). The experimentally observed characteristic features of the isomerization (the possibility of the Dimroth rearrangement occurring by the ANRORC mechanism and high energy barriers in acid-catalyzed reactions) were confirmed by quantum chemical calculations. Substituents in the triazole ring were found to play the principal role in the rearrangement.

Key words: 8,9,10,11-tetrahydrobenzo[*b*]thieno[2,3-*e*][1,2,4]triazolo[4,3-*c*]pyrimidines, Dimroth rearrangement, quantum chemical calculations.

The distinguishing feature of triazolopyrimidine systems is that they can be subjected to recyclization with various reagents or on exposure to heat or light.[1,2] The ability to be involved in these reactions is among the most characteristic properties of [1,2,4]triazolo[4,3-*c*]pyrimidines.[3]

As has been reported in several publications,[4—6] recyclizations (see Scheme 1) can be activated by both nucleophilic and electrophilic agents and involve approximately the same sequence of steps: addition of nucleophile (electrophile)—ring opening—ring closure (paths *A* and *B*).

The molecular mechanism involving the reaction of a heterocyclic substrate with a water molecule or simultaneously with H^+ and OH^- ions (path *C*) is also probable. However, we do not consider the latter mechanism because, as will be evident from the experimental data (see below), the rearrangement (see Scheme 1) can proceed as a typical acid- or base-catalyzed reaction (thermally and photochemically induced isomerizations are less preferable[7]).

In addition, the base-catalyzed pathway giving rise to the keto form in one of steps is presented at the center of Scheme 1. However, this pathway involves the 1,7-shift of the H atom from the N atom to the O atom attendant on the new ring closure, which evidently requires a considerable energy consumption in the case of an intramolecular reaction proceeding through the antiaromatic eight-center transition state.[8] For this reason, we do not consider this mechanism in the subsequent discussion.

The recyclization path *B* in Scheme 1 is the Dimroth rearrangement[2,9] occurring by the ANRORC mechanism.[2] Hence, the recyclization mechanism *A* can be arbitrarily called AERORC (addition of electrophile—ring opening—ring closure).

In the present study, we experimentally examined the possibility that isomerization might occur not only in an alkaline but also in an acidic medium (see Scheme 1, paths *B* and *A*, respectively) using the reactions of 8,9,10,11-tetrahydrobenzo[*b*]thieno[3,2-*e*][1,2,4]triazolo[1,5-*c*]pyrimidines **1a—e** and 8,9,10,11-tetrahydrobenzo[*b*]thieno[3,2-*e*][1,2,4]triazolo[4,3-*c*]pyrimidines **2a,b** as examples.

The reaction of 4-hydrazino-5,6,7,8-tetrahydrobenzo[4,5]thieno[2,3-*d*]pyrimidine (**3**) with triethyl orthoformate catalyzed by acetic acid was found to produce compound **2a** (Scheme 2). The reaction of aminoimines **4** affords products **1a—e**. Heating of acid chlorides with aminoimines **4** and hydrazines **3** in chlorobenzene in the presence of a catalytic amount of DMF gives rise to isomeric compounds **1c—e** and **2b**. However, unrearranged products for R = H (**2a**) or Me (**2b**) were prepared by acylation of hydrazines **3**. At the same time, starting from R = Et, the rearrangement into isomeric compounds **2c—e** occurs both in alkaline and acidic media.

Published in Russian in *Izvestiya Akademii Nauk. Seriya Khimicheskaya,* No. 12, pp. 2164—2171, December, 2006.

1066-5285/06/5512-2247 © 2006 Springer Science+Business Media, Inc.

Scheme 1

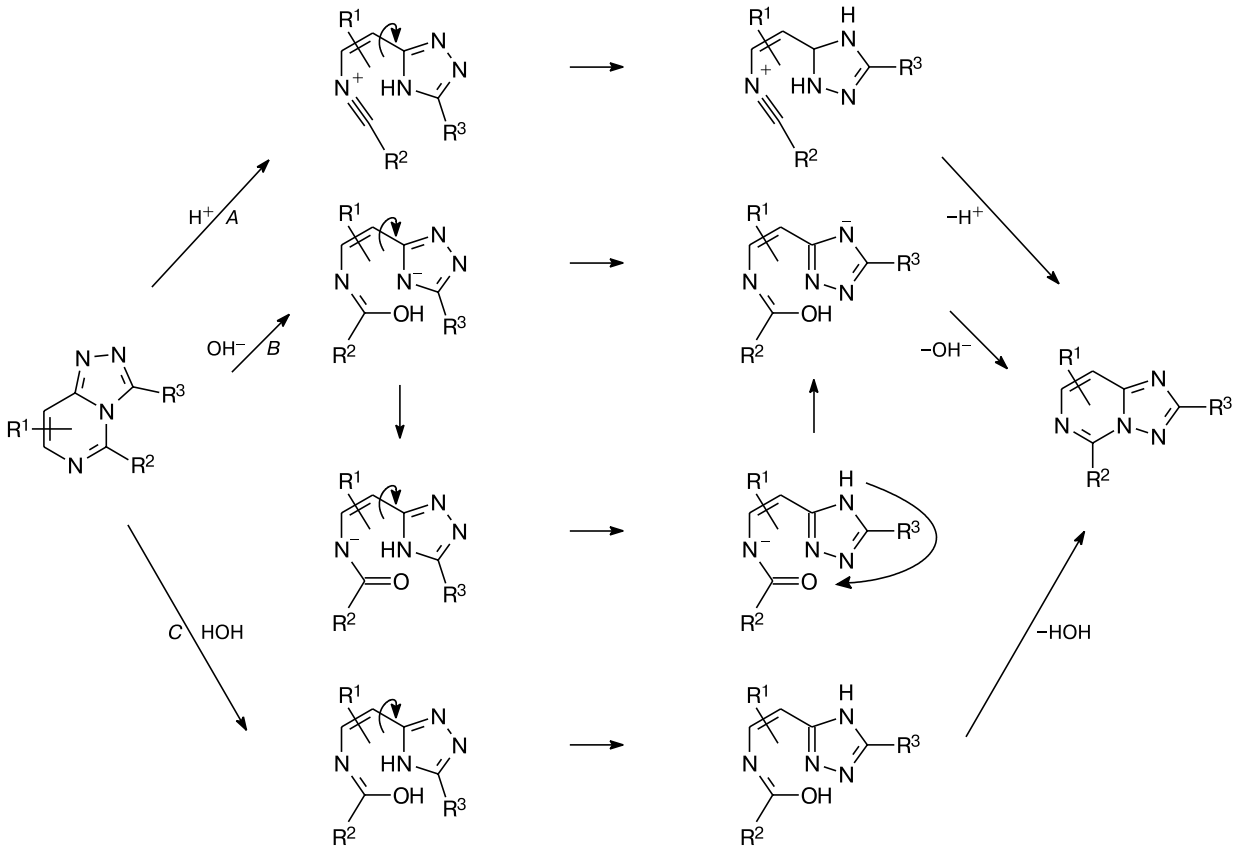

Scheme 2

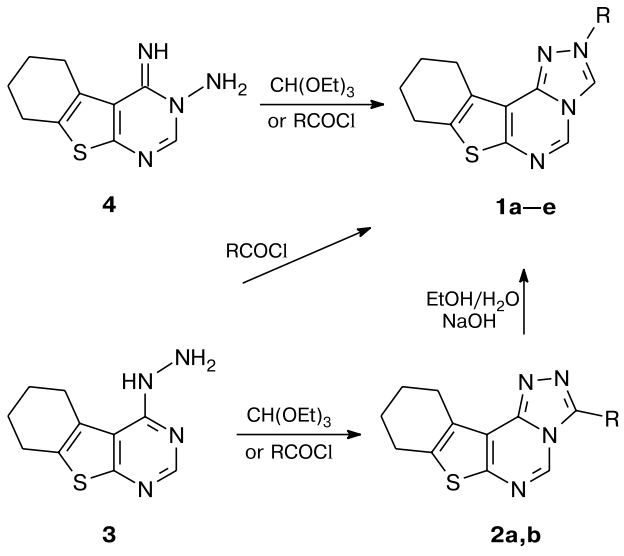

R = H (**a**), Me (**b**), Et (**c**), Pr (**d**), Bu (**e**)

All compounds were identified by ^{1}H NMR spectroscopy. Compounds **2a** and **2b** differ from compounds **1a** and **1b** by the chemical shifts of the signals for the H atoms in the pyrimidine and triazole rings, respectively. The signal for the pyrimidine proton in the spectra of all [1,2,4]triazolo[4,3-*c*]pyrimidines is observed at δ 9.0—9.3, whereas this signal in the spectra of [1,2,4]triazolo[1,5-*c*]pyrimidines appears at δ 8.4—8.6. In the spectra of [1,2,4]triazolo[1,5-*c*]pyrimidines, the signal of the substituents in the triazole ring is observed at higher field compared to that of isomeric [1,2,4]triazolo[4,3-*c*]pyrimidines.

Compounds **2a** and **2b** undergo the classical Dimroth rearrangement into compounds **1a** and **1b**, respectively, on refluxing in an aqueous ethanolic solution of an alkali.

Hence, the experimental data provide evidence that the isomerization mechanism depends not only on the acidity of the solution but also on the number of atoms in the carbon chain of the substituent R. At the same time, our results cannot be interpreted in favor of a particular rearrangement mechanism (see Scheme 1) and do not elucidate the nature of the dependence of the reaction rate on the substituent R. To solve this problem, we performed a detailed theoretical study of the isomerization mechanism taking into account both alternative cataly-

sis schemes and the length of the hydrocarbon substituent R.*

We carried out calculations for a model system (Scheme 3), which differs from the systems studied experimentally (see Schemes 1 and 2) in that it does not contain a substituent in the thiophene ring.

Scheme 3

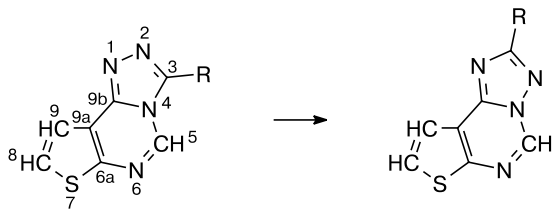

5 **6**

R = H, Me, Et, Pr, Bu

Rearrangement in an acidic medium

In terms of density functional theory (DFT), the electron chemical potentials μ, the chemical hardnesses η, and the global electrophilicity ω are used as efficient static descriptors (indices) for the prediction of the reactivity.[8] We calculated these characteristics for system **5** with R = C_nH_{2n+1}, where n = 0, 1, 2, 3, or 4 (the results are presented in Table 1).

Evidently, the electrophilicity ω gradually decreases and, consequently, the ability of system **5** to be protonated increases with increasing n. This is consistent with the experimental data on isomerization of compound **2a** in an acidic medium as the length of the carbon chain in the substituent R increases (acylation with acid chlorides leads to elimination of water and HCl, which remain in the reaction mixture and cause a shift of pH to acidic values; in the case of R = H, an acidic medium is produced by adding a catalytic amount of acetic acid).

The calculations also demonstrated that, at large distances, the reaction of **5** with such an electrophile as a proton is controlled by charges on atoms; at short distances, by the structure of the highest occupied molecular orbital HOMO of the substrate.[11] The Mulliken charges for the atoms in compound **5** (R = H) are presented in Fig. 1. The contributions of p_z-AO of the substrate to HOMO and the lowest unoccupied molecular orbitals (LUMO) are given in Table 2.

* It should be noted that, to our knowledge, quantum chemical calculations of the nucleophile-catalyzed isomerization (the Dimroth rearrangement) have been lacking in the literature. Evidently, the quantum chemical calculations performed in the study[10] are the exception.

Table 1. Electron chemical potentials (μ), the chemical hardnesses (η), and the global electrophilicity indices (ω) for system **5** with R = H, Me, Et, Pr, and Bu

R	−μ	η	ω
	eV		
H	4.1216	4.5626	1.8616
Me	3.9752	4.4732	1.7663
Et	3.9512	4.4684	1.7470
Pr	3.9423	4.4678	1.7392
Bu	3.9311	4.4510	1.7360

According to the calculations, at large distances (≥3 Å) from the triazole fragment, the proton is oriented mainly toward the N(4) atom bearing the highest negative charge (charge control), and approaches approximately perpendicular to the plane of the heterocycle. However, at a distance of ≤2.5 Å, the electrophile is reoriented from the N(4) atom to the nearest C(3) atom to form an intermediate, which is 42.9 kcal mol^{-1} more stable in the gas phase than the intermediate protonated at the N(4) atom (Table 3). This is consistent with the orbital control and is unexpected from the point of view of simple structural considerations. The relative energies of all competing cationic adducts and the lengths of the C(5)—N(4) bond, which is cleaved in the course of recyclization, are given in Table 3.

As can be seen from Table 3, protonation at the N(4) atom results in the loosening of the C(5)—N(4) bond that is cleaved in the course of recyclization, although this cation is energetically least stable of all the possible protonated forms. Hence, according to the calculations, the N(4) atom cannot be directly protonated. The only way of adding the proton to the N(4) atom is based on the migration from the C(3) atom. At the same time, deprotonation of another center adjacent to the N(4) atom, *viz.*, the C(5) atom, leads to migration of the proton not to the N(4) atom but to the N(6) atom (to form

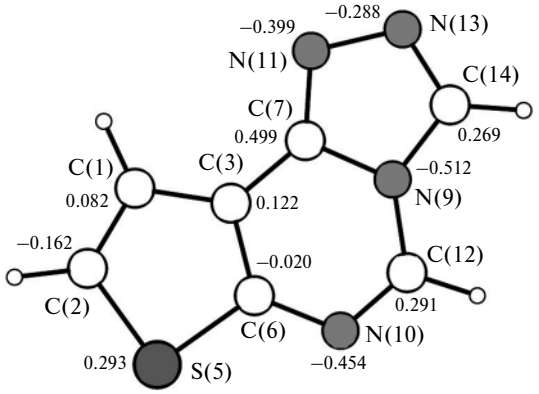

Fig. 1. Mulliken charges for the atoms in compound **5** (R = H).

Table 2. Contributions of p_z-AO to the frontier MO of system **5** with R = H, Me, Et, Pr, and Bu

Atom	HOMO					LUMO				
	H	Me	Et	Pr	Bu	H	Me	Et	Pr	Bu
N(1)	+0.21	+0.22	+0.22	+0.21	+0.21	−0.04	−0.04	−0.04	−0.04	−0.04
N(2)	−0.03	−0.06	−0.06	−0.06	−0.06	+0.16	+0.16	+0.15	+0.15	+0.15
C(3)	+0.19	+0.18	+0.18	+0.17	+0.17	−0.07	−0.07	−0.07	−0.07	−0.07
N(4)	−0.05	−0.07	−0.07	−0.07	−0.06	−0.15	−0.15	−0.15	−0.15	−0.14
C(5)	+0.16	+0.16	+0.16	+0.16	+0.16	+0.40	+0.41	+0.41	+0.41	+0.42
N(6)	+0.08	+0.07	+0.08	+0.08	+0.08	−0.24	−0.24	−0.24	−0.23	−0.23
C(6a)	−0.22	−0.21	−0.21	−0.21	−0.2	−0.20	−0.21	−0.21	−0.22	−0.22
S(7)	+0.08	+0.11	+0.12	+0.14	+0.16	+0.24	+0.23	+0.23	+0.23	+0.23
C(8)	+0.19	+0.17	+0.17	+0.16	+0.16	−0.29	−0.29	−0.29	−0.28	−0.28
C(9)	+0.05	+0.03	+0.02	+0.02	+0.02	+0.08	+0.08	+0.08	+0.08	+0.08
C(9a)	−0.16	−0.16	−0.16	−0.16	−0.16	+0.27	+0.26	+0.26	+0.25	+0.25
C(9b)	+0.08	+0.10	+0.11	+0.13	+0.14	−0.11	−0.11	−0.10	−0.09	−0.09

Table 3. Energy and geometric characteristics of the possible adducts of **5** (R = H) with a proton*

Protonation site	$-E_{rel}$ /kcal mol^{-1}	C(5)—N(4) Bond length /Å
N(1)—H	75.1	1.394
C(3)—H	42.9	1.363
N(4)—H	0.0	1.543
C(5)—H	27.7	1.472
C(6a)—H	27.5	1.412
C(8)—H	37.7	1.361
C(9a)—H	21.9	1.361

* The atomic numbering scheme is presented in Fig. 1. The energy of the substrate protonated at the N(4) atom was taken as the reference point.

another cation, in which the N(4)—C(5) bond length (1.330 Å) is very small), the process being characterized by a high energy barrier (61.8 kcal mol^{-1} in the gas phase).

Hence, the reaction (Scheme 4) involves protonation not of the heteroatoms of the substrate but of the C(3) atom as the first step followed by the 1,2-shift of the proton to the N(4) atom, which sets the stage for the third step of the reaction, *viz.*, the ring opening at the C(5)—N(4) bond, followed by the steps according to Scheme 1 (path *A*). Therefore, the rearrangement mechanism shown in Scheme 4 can be proposed for the compounds under consideration.

As expected, the attack of a proton on the C(3) atom to form cation **7** is barrierless, whereas the 1,2-sigmatropic shift giving rise to intermediate **8** requires a considerable energy consumption (81.9 kcal mol^{-1} in the gas phase, Figs 2 and 3).

It should be noted that the formation of cation **8** is accompanied by a considerable acoplanarity of the bonds at the N(4) atom, which deviates from the common plane of the annulated rings by 0.401 Å. The subsequent opening of the pyrimidine ring at the C(5)—N(4) bond occurs

Scheme 4

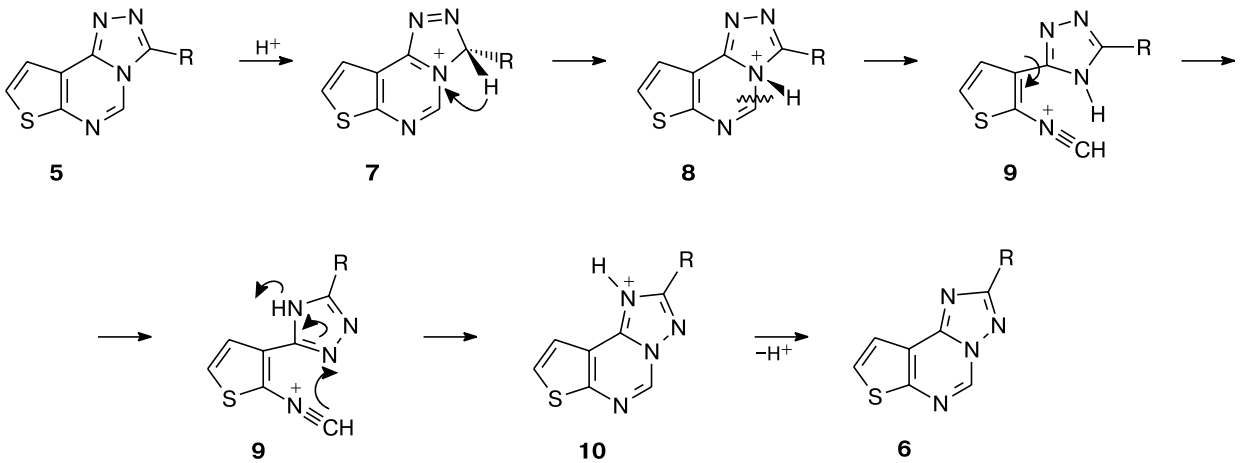

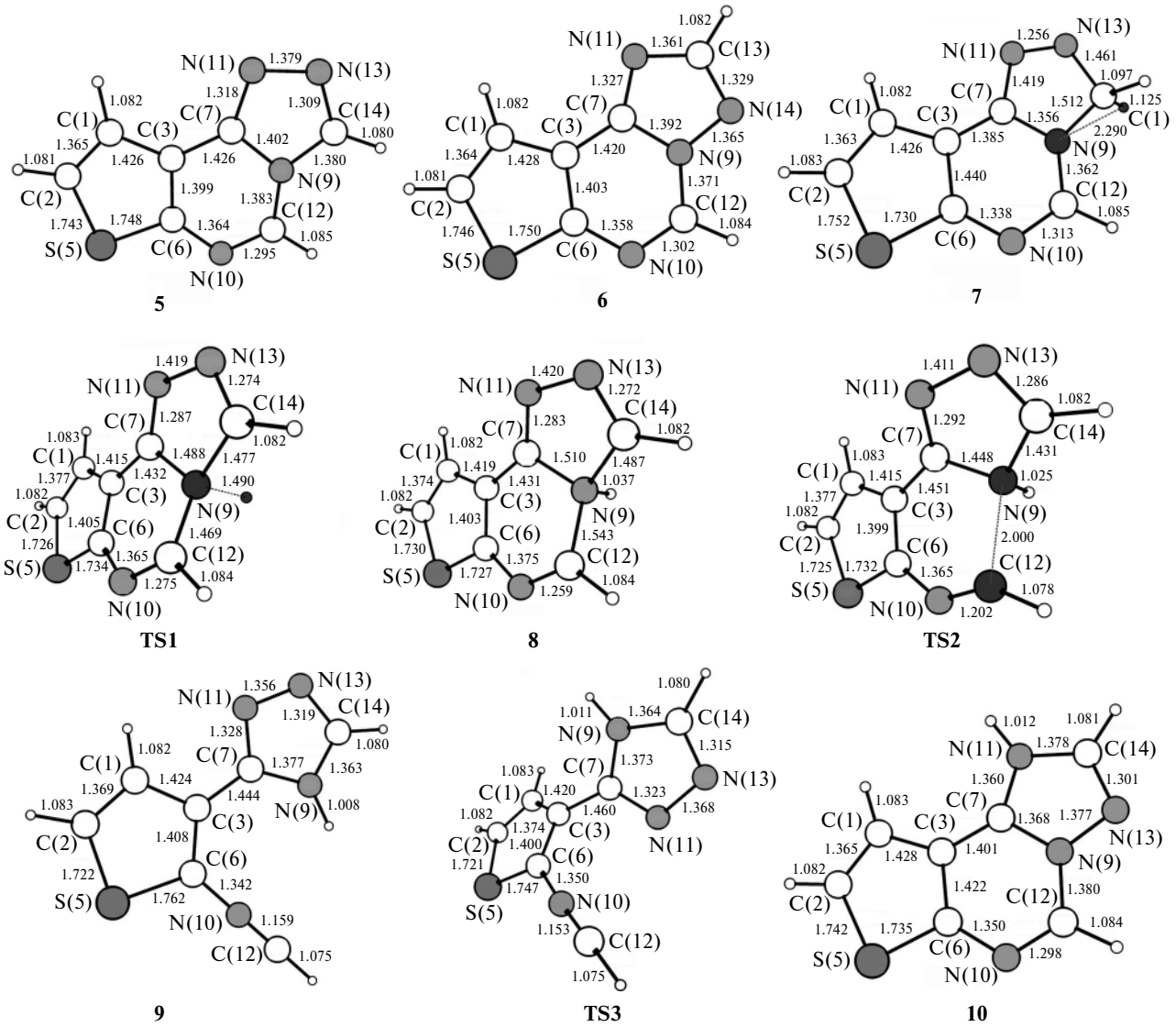

Fig. 2. Calculated geometric characteristics of the stationary points along the minimum-energy reaction path (see Scheme 4); the bond lengths (Å) are given.

already with a small energy barrier (4.7 kcal mol^{-1}) and gives intermediate **9** (see Fig. 3).

Interestingly, the energy progressively decreases in the successive steps of conformational rotation (**9** → **9a**) and cyclization up to the formation of cation **10**, which is exceptionally stable in the gas phase (see Fig. 3).

We also took into account the solvation effects in the acid-catalyzed rearrangement in terms of the polarizable continuum model (see Fig. 3, Table 4).

The calculations demonstrated that the sequence of steps of the process **5** → **6** in solution is identical to that in the gas phase, whereas the energy barriers are somewhat lower (for example, the 1,2-shift of the proton from the C(5) atom to the N(4) atom, which is the rate-determining step, is accompanied by a decrease in the activation barrier by 11.6 kcal mol^{-1}).

On the whole, it can be concluded that already the first step of the electrophilic attack on system **5** both in the gas phase and in solution affords intermediate **7**, which is both thermodynamically and kinetically stable to further isomerization, and this excludes the acid-catalyzed rearrangement **5** → **6**.

Rearrangement in an alkaline medium

In the reaction in an alkaline medium, unlike that in an acidic medium, the nucleophilic attack on the electron-deficient C(5) atom located between two electronegative nitrogen atoms, N(4) and N(6), would be expected to occur already in the first step. This gives rise to anion **11**, and its subsequent reorganization is described by Scheme 5 (Fig. 4).

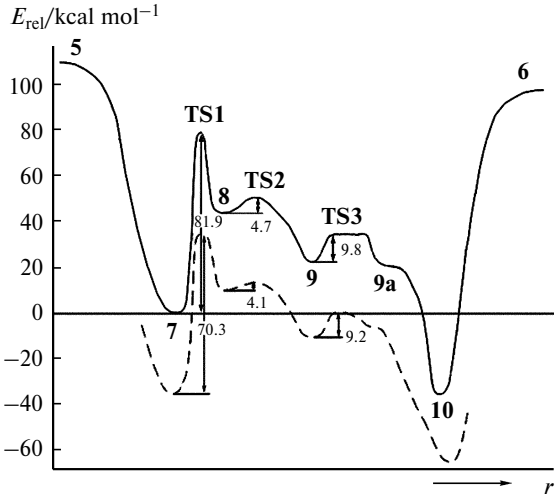

Fig. 3. Potential energy surface along the minimum-energy path for the proton-catalyzed rearrangement **5** → **6** in the gas phase (solid line) and in solution (dashed line); *r* is the reaction coordinate.

Table 4. Total energies (E_{tot}), the relative total energies (E_{rel}), and the Gibbs free energies (ΔG) calculated for the gas phase of systems **5** (R = H), **7**, **8**, and **10** and the relative Gibbs free energies calculated with inclusion of the solvent effect (ΔG_{solv})*

System	$-E_{tot}$ /au	$-E_{rel}$	$-\Delta G$	$-\Delta G_{solv}$
		kcal mol^{-1}		
7	886.65267	208.1	110.3	237.9
TS1	886.52220	126.2	86.6	166.8
8	886.58022	162.6	94.6	192.2
TS2	886.57273	157.9	95.6	191.6
10	886.70620	241.7	120.2	268.1
5 + H^+	886.49385	108.4	48.3	8.6

* For all stationary points for the minimum-energy reaction path (see Scheme 4), the ZPE-corrected total energies of the structures, and the relative energies for standard conditions (1 atm and 298 K) are given.[10,11] The total energy of compound **5** (R = H) and a proton at an infinite distance from each other was taken as the reference point.

The formation of anion **11** is accompanied by a monotonous decrease in the total energy of the system both in the gas phase and in solution (Fig. 5, Table 5), and the attack occurs in the direction of the maximum interaction between HOMO of the OH^- ion and LUMO of the substrate, the contribution of the C(5) atom to the latter being maximum for all the substituents R under consideration (see Table 2).

The energy barriers for all intermediate steps of the ANRORC process are rather low already in the gas phase. Taking into account the solvent effect, all stationary points are stabilized and the activation barriers are slightly decreased. Hence, the ANRORC path of the rearrangement is evidently the only possible path for system **5** with R = H.

To summarize, the quantum chemical DFT calculations showed that the isomerization **5** → **6** can be considered as a typical Dimroth rearrangement occurring by the ANRORC mechanism. The electrophilic attack followed by isomerization (arbitrarily, the AERORC path) implies that the 1,2-sigmatropic shift of hydrogen in the protonated substrate is the rate-determining step, which completely excludes this recyclization for R = H.

At the same time, the probability of the direct electrophilic attack on the N(4) atom of the substrate in the AERORC path increases with increasing number of C atoms in the substituent R in the series R = H, Me, Et, Pr, and Bu (see Table 1), due to which this competitive path becomes more probable and, consequently, the rearrangement **5** → **6** can occur not only in an alkaline but also in an acidic medium. This conclusion is completely consistent with the experimental data for the isomerizations **2a** → **1a** and **2b** → **1b**.

Scheme 5

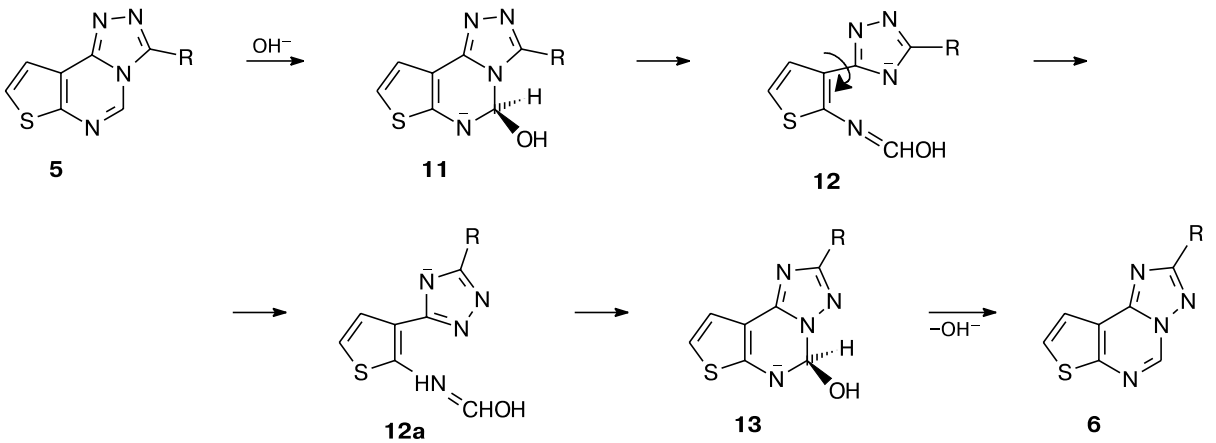

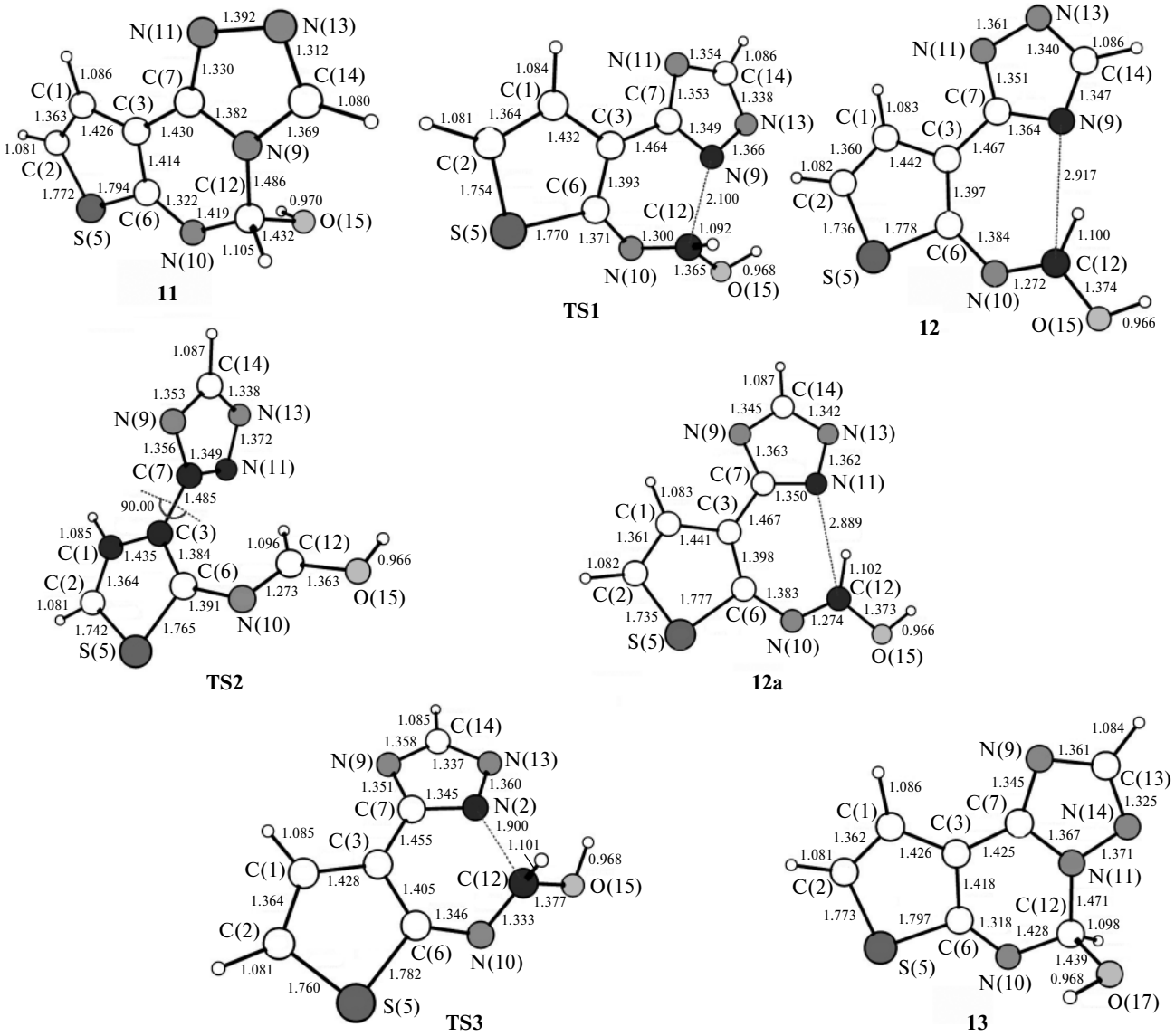

Fig. 4. Calculated geometric characteristics of the stationary points along the minimum-energy reaction path (see Scheme 5); the bond lengths (Å) and bond angles (deg) are given.

Experimental

The ^{1}H NMR spectra were recorded on Bruker DPX-250 (250 MHz) and Varian Unity-300 (300 MHz) instruments in $CDCl_3$ with Me_4Si as the internal standard. The IR spectra were measured on a Specord IR-75 spectrometer in Nujol mulls. The electron-impact mass spectra were obtained on a Finnigan Mat Incos 50 instrument using a direct inlet system; the ionizing voltage was 70 V. The chromatographic purification was performed on Al_2O_3 using $CHCl_3$ as the eluent.

3-Amino-4-imino-5,6,7,8-tetrahydrobenzo[4,5]thieno-[2,3-*d*]pyrimidine (4) was synthesized according to a procedure described earlier.[12]

4-Hydrazino-5,6,7,8-tetrahydrobenzo[4,5]thieno[2,3-*d*]-pyrimidine (3). Aminoimine **4** (22 g, 0.1 mol) was refluxed in an aqueous ethanolic solution (water, 75 mL; EtOH, 75 mL) in the presence of NaOH (20 mg) for 48 h and concentrated to dryness. Then EtOH (25 mL) was added. After 12 h, the precipitate that formed was filtered off and washed with petroleum ether. The yield was 20.9 g (95%), m.p. 106—108 °C. Found (%): C, 54.53; H, 5.94; N, 24.96; S, 13.75. $C_{10}H_{12}N_4S$. Calculated (%): C, 54.55; H, 5.45; N, 25.45; S, 14.55. ^{1}H NMR, δ: 1.98 (t, 4 H, CH_2, J = 5.5 Hz); 2. 94 (m, 4 H, CH_2); 4.12 (d, 2 H, NH_2, J = 8.5 Hz); 6.47 (t, 1 H, NH, J = 6.0 Hz); 8.47 (s, 1 H, CH).

8,9,10,11-Tetrahydrobenzo[4,5]thieno[3,2-*e*][1,2,4]triazo-lo[1,5-*c*]pyrimidine (1a) and **8,9,10,11-tetrahydrobenzo[4,5]-thieno[3,2-*e*][1,2,4]triazolo[4,3-*c*]pyrimidine(2a). Method *A*.** A solution of aminoimine **4** (0.01 mol) (hydrazine **3** for the synthesis of compound **2a**), triethyl orthoformate (4 mL, 0.05 mol), and AcOH (10 mol.%) was refluxed for 2 h, purified by column chromatography, recrystallized from EtOH, filtered off, and washed with EtOH.

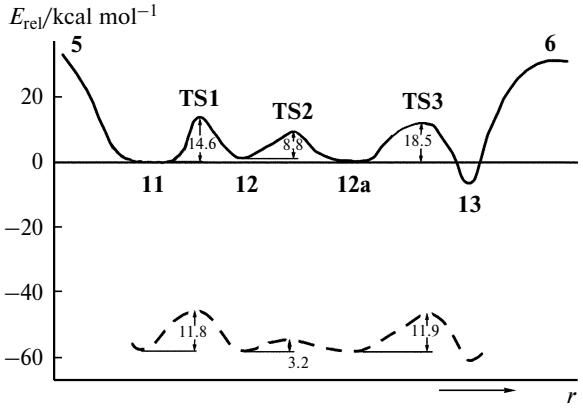

Fig. 5. Potential energy surface along the minimum-energy path for the hydroxide-catalyzed rearrangement **5** → **6** in the gas phase (solid line) and in solution (dashed line); *r* is the reaction coordinate.

Table 5. Total energies (E_{tot}), the relative total energies (E_{rel}), and the Gibbs free energies (ΔG) calculated for the gas phase of systems **6** (R = H) and **11**—**13** and the relative Gibbs free energies calculated with inclusion of the solvent effect (ΔG_{solv})*

System	$-E_{tot}$ /au	$-E_{rel}$	$-\Delta G$	$-\Delta G_{solv}$
		kcal mol^{-1}		
11	962.18975	89.6	38.3	29.3
TS1	962.17131	78.0	24.0	17.7
12	962.18687	87.8	37.8	29.8
TS2	962.17452	80.0	29.5	25.8
12a	962.18855	88.8	38.9	29.9
TS3	962.17029	77.4	26.6	18.2
13	962.19971	95.8	44.0	33.0
6 + OH^-	962.13951	58.0	8.7	14.4

* Transition states **TS1**—**TS3** are presented in Fig. 4. The total energy of compound **5** (R = H) and a hydroxide anion at an infinite distance from each other was taken as the reference point.

Method *B* (Dimroth rearrangement of compounds 2a,b). Compounds **2a,b** (0.01 mol) were refluxed in an aqueous ethanolic solution (water, 75 mL; EtOH, 75 mL) in the presence of NaOH (20 mg) for 48 h and concentrated to dryness. Then EtOH (25 mL) was added. After 12 h, the precipitate was filtered off and washed with petroleum ether.

8,9,10,11-Tetrahydrobenzo[4,5]thieno[3,2-*e*][1,2,4]triazolo[1,5-*c*]pyrimidine (1a). The yield was 2.11 g (92%, *A*) and 1.83 g (80%, *B*), m.p. 132—134 °C (*cf.* lit. data[13]: m.p. 138—139 °C). Found (%): C, 57.09; H, 4.65; N, 24.75; S, 14.12. $C_{11}H_{10}N_4S$. Calculated (%): C, 57.39; H, 4.35; N, 24.35; S, 13.91. ^{1}H NMR, δ: 2.00 (t, 4 H, CH_2, J = 5.5 Hz); 2.96 and 3.18 (both m, 2 H each, CH_2); 8.41 and 9.18 (both s, 1 H each, CH).

8,9,10,11-Tetrahydrobenzo[4,5]thieno[3,2-*e*][1,2,4]triazolo[4,3-*c*]pyrimidine (2a). The yield was 2.05 g (89%), m.p. 289—292 °C (*cf.* lit. data[13]: m.p. 306—308 °C). Found (%): C, 57.02; H, 4.67; N, 24.74; S, 14.15. $C_{11}H_{10}N_4S$. Calculated (%): C, 57.39; H, 4.35; N, 24.35; S, 13.91. ^{1}H NMR, δ: 1.98 (t, 4 H, CH_2, J = 5.5 Hz); 2.95 and 3.16 (both m, 2 H each, CH_2); 9.22 and 9.30 (both s, 1 H each, CH).

8,9,10,11-Tetrahydrobenzo[4,5]thieno[3,2-*e*][1,2,4]triazolo[1,5-*c*]pyrimidines 1b—e and 8,9,10,11-tetrahydrobenzo[4,5]thieno[3,2-*e*][1,2,4]triazolo[4,3-*c*]pyrimidine (2b). A suspension of the starting acid (0.01 mol), thionyl chloride (0.72 mL, 0.01 mol), and DMF (10 mol.%) in chlorobenzene (20 mL) was refluxed until elimination of HCl ceased. Then aminoimine **4** was added for the preparation of **1b—e** (hydrazine **3** was added for the preparation of **1b—e** and **2b**). The reaction mixture was refluxed for 4 h, extracted with chloroform (3×20 mL) and a 15% aqueous ammonia solution (3×20 mL), purified by column chromatography, recrystalized from EtOH, filtered off, and washed with EtOH.

2-Methyl-8,9,10,11-tetrahydrobenzo[4,5]thieno[3,2-*e*][1,2,4]triazolo[1,5-*c*]pyrimidine (1b). The yield was 1.66 g (68%, *A*) and 1.76 g (72%, *B*), m.p. 160—162 °C. Found (%): C, 58.92; H, 4.94; N, 22.91; S, 13.14. $C_{12}H_{12}N_4S$. Calculated (%): C, 59.02; H, 4.92; N, 22.95; S, 13.11. ^{1}H NMR, δ: 1.97 (m, 4 H, CH_2); 2. 68 (s, 3 H, Me); 2.95 (t, 2 H, CH_2, J = 5.5 Hz); 3.20 (t, 2 H, CH_2, J = 6.0 Hz); 9.07 (s, 1 H, CH).

3-Methyl-8,9,10,11-tetrahydrobenzo[4,5]thieno[3,2-*e*][1,2,4]triazolo[4,3-*c*]pyrimidine (2b). The yield was 1.44 g (59%, *A*), m.p. 195—197 °C. Found (%): C, 59.00; H, 4.93; N, 22.91; S, 13.12. $C_{12}H_{12}N_4S$. Calculated (%): C, 59.02; H, 4.92; N, 22.95; S, 13.11. ^{1}H NMR, δ: 2.01 (m, 4 H, CH_2); 2. 878 (s, 3 H, Me); 2.94 (t, 2 H, CH_2, J = 5.7 Hz); 3.30 (t, 2 H, CH_2, J = 6.3 Hz); 8.60 (s, 1 H, CH).

2-Ethyl-8,9,10,11-tetrahydrobenzo[4,5]thieno[3,2-*e*][1,2,4]triazolo[1,5-*c*]pyrimidine (1c). The yield was 1.81 g (70%, *A*) and 1.91 g (74%, *B*), m.p. 118—120 °C. Found (%): C, 60.41; H, 5.49; N, 21.68; S, 12.41. $C_{13}H_{14}N_4S$. Calculated (%): C, 60.47; H, 5.43; N, 21.71; S, 12.40. ^{1}H NMR, δ: 1.42 (t, 3 H, Me, J = 10.5 Hz); 1.95 (m, 4 H, CH_2); 2.96 (t, 2 H, CH_2, J = 6.5 Hz); 3.05 (m, 2 H, CH_2); 3.21 (t, 2 H, CH_2, J = 6.3 Hz); 9.09 (s, 1 H, CH).

2-Propyl-8,9,10,11-tetrahydrobenzo[4,5]thieno[3,2-*e*][1,2,4]triazolo[1,5-*c*]pyrimidine (1d). The yield was 1.79 g (66%, *A*) and 1.85 g (68%, *B*), m.p. 99—100 °C. Found (%): C, 61.67; H, 5.89; N, 20.55; S, 11.78. $C_{14}H_{16}N_4S$. Calculated (%): C, 61.76; H, 5.88; N, 20.59; S, 11.76. ^{1}H NMR, δ: 1.07 (t, 3 H, Me, J = 9.7 Hz); 1.95 (m, 2 H, CH_2); 2.02 (t, 4 H, CH_2, J = 6.8 Hz); 2.97 (m, 4 H, CH_2); 3.20 (t, 2 H, CH_2, J = 5.9 Hz); 9.06 (s, 1 H, CH).

2-Butyl-8,9,10,11-tetrahydrobenzo[4,5]thieno[3,2-*e*][1,2,4]triazolo[1,5-*c*]pyrimidine (1e). The yield was 1.80 g (63%, *A*) and 2.0 g (70%, *B*), m.p. 83—84 °C. Found (%): C, 62.87; H, 6.31; N, 22.94, S, 11.19. $C_{15}H_{18}N_4S$. Calculated (%): C, 62.94; H, 6.29; N, 22.95; S, 11.19. ^{1}H NMR, δ: 0.98 (t, 3 H, Me, J = 9.6 Hz); 1.42 and 1.85 (both m, 2 H each, CH_2); 1.91 (t, 4 H, CH_2, J = 7.8 Hz); 2.95 (m, 4 H, CH_2); 3.20 (t, 2 H, CH_2, J = 5.5 Hz); 9.07 (s, 1 H, CH).

All calculations were performed by density functional theory (DFT) with the Becke3LYP three-parameter hybrid functional[14] and the 6-31G** basis set.[15]

Calculations were carried out with the use of the GAUSSIAN-98 program package.[16] The final full geometry optimization of the molecular structures corresponding to stationary points on the potential energy surface was performed using the tight-binding method and the GAUSSIAN-98 program

package. If necessary, the synchronous transit method[17] was used for searching the transition state structures. The structures corresponding to minima on the potential energy surface were found by the steepest descent method from each saddle point.

The solvation effects for an ethanolic medium were taken into account with the use of single-point (without geometry optimization) B3LYP/6-31G** calculations of the gas-phase structures and the self-consistent reaction field (SCRF)[18] based on the polarizable continuum model (PCM).[19]

References

1. *Comprehensive Organic Chemistry*, Eds D. Barton and W. D. Ollis, Pergamon Press, Oxford, 1979, Vol. **2**.
2. A. F. Pozharskii, *Teoreticheskie osnovy khimii geterotsiklov* [*Theoretical Fundamentals of Chemistry of Heterocycles*], Khimiya, Moscow, 1985, p. 278 (in Russian).
3. D. J. Brown, *Mechanisms of Molecular Migrations*, New York, 1968, Vol. **1**, 209.
4. N. Guillot, H. G. Viehe, B. Tinant, and J. P. Declercq, *Tetrahedron*, 1990, **46**, 3897.
5. D. J. Brown and T. Nagamatsu, *Aust. J. Chem.*, 1977, **30**, 2515.
6. D. J. Brown and T. Nagamatsu, *Aust. J. Chem.*, 1978, **31**, 2505.
7. G. G. Danagulyan, L. G. Saakyan, and M. G. Zalinyan, *Khim. Geterotsikl. Soedin.*, 1992, 225 [*Chem. Heterocycl. Compd.*, 1992 (Engl. Transl.)].
8. V. I. Minkin, B. Ya. Simkin, and R. M. Minyaev, *Kvantovaya khimiya organicheskikh soedinenii. Mekhanizmy reaktsii* [*Quantum Chemistry of Organic Compounds: Reaction Mechanisms*], Khimiya, Moscow, 1986, 248 pp. (in Russian).
9. P. J. Robinson, *J. Chem. Educ.*, 1978, **55**, 509.
10. Yu. O. Subbotina, Ph. D. (Chem.) Thesis, Ural State Technical University, Ekaterinburg, 2005, 183 pp. (in Russian).
11. W. M. F. Fabian, *J. Org. Chem.*, 2002, **67**, 7475.
12. F. Sauter and P. Stanetty, *Monatsh. Chem.*, 1975, **106**, 1111.
13. C. J. Shishoo, M. B. Devani, G. V. Ullas, S. Ananthan, and V. S. Bhadi, *J. Heterocycl. Chem.*, 1981, **18**, 43.
14. N. D. Chuvylkin, *Zh. Vsesoyuz. Khim. Obshch. im. D. I. Mendeleeva*, 1990, **35**, 660 [*Mendeleev Chem. J.*, 1990, **35** (Engl. Transl.)].
15. J. B. Foresman and E. Frisch, *Exploring Chemistry with Electronic Structure Methods*, Gaussian, Inc., Pittsburgh (PA), 2nd ed., 1996, 302.
16. M. J. Frisch, G. W. Trucks, H. B. Schlegel, G. E. Scuseria, M. A. Robb, J. R. Cheeseman, V. G. Zakrzewski, J. A. Montgomery, Jr., R. E. Stratmann, J. C. Burant, S. Dapprich, J. M. Millam, A. D. Daniels, K. N. Kudin, M. C. Strain, O. Farkas, J. Tomasi, V. Barone, M. Cossi, R. Cammi, B. Mennucci, C. Pomelli, C. Adamo, S. Clifford, J. Ochterski, G. A. Petersson, P. Y. Ayala, Q. Cui, K. Morokuma, D. K. Malick, A. D. Rabuck, K. Raghavachari, J. B. Foresman, J. Cioslowski, J. V. Ortiz, A. G. Baboul, B. B. Stefanov, G. Liu, A. Liashenko, P. Piskorz, I. Komaromi, R. Gomperts, R. L. Martin, D. J. Fox, T. Keith, M. A. Al-Laham, C. Y. Peng, A. Nanayakkara, M. Challacombe, P. M. W. Gill, B. Johnson, W. Chen, M. W. Wong, J. L. Andres, C. Gonzalez, M. Head-Gordon, E. S. Replogle, and J. A. Pople, *GAUSSIAN*, Gaussian Inc., Pittsburgh (PA), 1998.
17. T. A. Halgren and W. N. Lipscomb, *Chem. Phys. Lett.*, 1977, **49**, 225.
18. B. Y. Simkin and I. Sheikhet, *Quantum Chemical and Statistical Theory of Solutions: A Computational Approach*, Ellis Horwood, London, 1995.
19. V. Barone, M. Cossi, and J. Tomasi, *J. Comput. Chem.*, 1998, **19**, 404.

Received July 26, 2006;
in revised form September 27, 2006